

# UC San Diego

## UC San Diego Electronic Theses and Dissertations

### Title

A novel maize 9-allene oxide cyclase (9-AOC) is required for the biosynthesis of protective Death Acid (DA) defenses

### Permalink

<https://escholarship.org/uc/item/0jz8v69p>

### Author

Dadafshar, Armin

### Publication Date

2021

Peer reviewed|Thesis/dissertation

UNIVERSITY OF CALIFORNIA SAN DIEGO

A novel maize 9-allene oxide cyclase (9-AOC) is required  
for the biosynthesis of protective Death Acid (DA) defenses

A Thesis submitted in partial satisfaction of the requirements for the degree Master of

Science

in

Biology

by

Armin Dadafshar

Committee in charge:

Professor Eric Schmelz, Chair

Professor Alisa Huffaker, Co-Chair

Professor Jose Pruneda-Paz

2021

Copyright

Armin Dadafshar, 2021

All rights reserved.

The Thesis of Armin Dadafshar is approved, and it is acceptable in quality and form for publication on microfilm and electronically.

University of California San Diego

2021

## TABLE OF CONTENTS

Thesis Approval Page .....	iii
Table of Contents .....	iv
List of Figures .....	v
List of Tables .....	vi
Acknowledgements .....	vii
Abstract of the Thesis .....	ix
Introduction.....	1
Materials and Methods.....	8
Results.....	17
Discussion.....	32
References.....	40

## LIST OF FIGURES

Figure 1: Combined linkage and association mapping identifies a locus on chromosome 6 regulating 10-oxo-11-phytoenoic acid (10-OPEA) concentrations .....	23
Figure 2: Phylogenetic and expression analysis of the maize germin-like family genes .....	24
Figure 3: A maize germin-like protein (GLP) functions as a 9-AOC for Death Acid biosynthesis.....	25
Figure 4: Maize terpenoid phytoalexin production in scutella tissues are not inhibited in <i>9-aoc</i> mutant .....	27
Figure 5: Maize <i>9-aoc</i> mutants lack accumulation of Death Acids in B73 scutella .....	28
Figure 6a: Maize <i>9-aoc</i> mutants lack fungal elicited production of the linoleic acid (18:2) derived death acid 10-OPEA.....	29
Figure 6b: Maize <i>9-aoc</i> mutants lack fungal elicited production of the linolenic acid (18:3) derived death acid, 10-oxo 11-phytodienoic acid (10-OPDA) .....	30
Figure 7: Maize <i>9-aoc</i> mutants are not compromised in the fungal-elicited production of zealexins in stems .....	31

## LIST OF TABLES

Table 1: GWAS mapping interval identified using 10-OPEA levels as a metabolic trait in the Goodman association panel and SLB-elicited leaf transcript levels (24h post inoculation) as a filter in the consideration of gene candidates .....	26
---	----

## ACKNOWLEDGMENTS

First and foremost, I would like to thank my amazing Mom and Dad who were always supporting me in my educational endeavors and pushing me to always strive farther. Like most immigrants, my parents sacrificed their own lives to come start anew in search of a better opportunity for me and my siblings. In May 2019, my mother was diagnosed with breast cancer. It felt that everything we had done to this point was meaningless. As my Mom called me crying after being told the drastic news, I did whatever I could to take away from this serious disease and give her hope daily. Just like how my Mom was there for me every second, through thick and thin, I made sure to dedicate all of my time to help her fight and win. One day we got news that her cancer had spread to her lungs. Coincidentally, that day was the day I got notice that I had been accepted in to the BS/MS program and would be starting my Masters. I didn't know how to give her hope as the doctors were very straight-forward with the new diagnosis. I'll never forget when I told her that I was just admitted... her face was filled with joy and proceeded to tell me that because I was always helping her with everything, God made this happen. She asked when do you finish and I told her a month after your birthday in May... I just can't believe that she isn't here to see this and be part of another graduation. I dedicate this for my Mom. Thank you for everything you did for me. I hope to continue to make you proud.....

I want to greatly thank my thesis advisor and mentor Dr. Eric A. Schmelz for being so helpful and patient with me. Ever since I started this program it has been hard to mentally adjust after losing my Mom but he was very understanding and accommodating.

He gave me the opportunity back in December 2018 and although I started off roughly I hope I was able to contribute at a much greater level. I remember that Zoom talk we had right after I lost my Mom which was a very dear conversation to me. I tried to take that advice and use research to distract me and although I wanted to leave everything behind, I somehow was able to put in my time in lab and try to focus. I know there was a lot of work that needed to be done but regardless Dr. Schmelz always took into consideration what I was going through and worked around me a lot and I sincerely appreciate that. Dr. Yezhang Ding and visiting scholar Mengxi Wu were a source of massive patience, expertise, and leadership on much of surrounding efforts enabling discovery and proof of the 9-allene oxide cyclase in maize. It goes without saying that my project simply would not have been possible without Dr. Schmelz, Dr. Ding and Mengxi Wu whose passion for the research concepts preceded my time in the lab and continued for its duration. Research contributions of Dr. Ding are noted specifically in the Master thesis to clearly delineate contributions that were essential to include for the logic flow and research narrative. Furthermore I want to give a massive thank you to Ahmed Khalil, who played an important role in me being on top of my work and getting things done. Anytime I had a question he would be quick to jump in and help or make sure I understand a concept. I tried to be as independent as I could, but I know I annoyed him a fair share throughout my time here. He made being in lab a very fun and welcoming place with his positive attitude and corny jokes. Last but not least, I want to thank Calvin Harris and Aysha Alani for helping me on some of my experiments and enabling me to have an extra two sets of hands when one wasn't enough.

## ABSTRACT OF THE THESIS

A novel maize 9-allene oxide cyclase (9-AOC) is required for the biosynthesis of protective Death Acid (DA) defenses

by

Armin Dadafshar

Master of Science in Biology

University of California San Diego, 2021

Professor Eric Schmelz, Chair

Professor Alisa Huffaker, Co-Chair

In plants, the precise regulation of cell survival or cell death decisions control effective immunity to different types of pathogens. Cellular damage in plants results in the enzymatic and non-enzymatic peroxidation of fatty acids known as oxylipins. Enzymatic oxylipin biosynthesis often begins with the lipase-based cleavage of linoleic (18:2) or linolenic acid (18:3) from membrane bound lipids. Fatty acids are then

dioxygenated by lipoxygenases (LOXs) with regiospecificity at carbons 9 (9-LOX) or 13 (13-LOX) resulting in unstable fatty acid hydroperoxides. Specific oxylipins serve as direct antimicrobial defenses and plant signaling molecules regulating diverse processes such as development, stress acclimation and innate immune responses against pests and pathogens. A commonly studied enzymatic pathway for the 13-LOX 18:3 fatty acid product, termed 13(S)-hydroperoxylinolenic acid, is the sequential activity of 13-allene oxide synthase (13-AOS) and 13-allene oxide cyclase (13-AOC) to yield 12,13(S)-epoxylinolenic acid and finally the 18-carbon cyclopentenone termed 12-oxo-phytodienoic acid (12-OPDA). 12-OPDA is an essential precursor to the 12-carbon cyclopentanone termed jasmonic acid (JA), an essential precursor to the plant hormone JA-isoleucine that controls defense activation and reproduction. In maize (*Zea mays*) leaves, southern leaf blight (SLB; *Cochliobolus heterostrophus*) infection results in the additional accumulation of jasmonate-like positional isomers derived from the activity of 9-LOX. These molecules include 10-oxo-11-phytodienoic acid (10-OPDA) and 10-oxo-11-phytoenoic acid (10-OPEA), derived from 18:3 and 18:2 respectively, and the respective series of 14- and 12- carbon metabolites termed death acids (DA). The accumulation of 10-OPEA becomes wound-inducible in fungal-infected maize tissues, is phytotoxic and acts as a direct defense suppressing fungal growth [1]. Conceptually DAs are predicted to be derived from 9-LOX, 9-AOS and novel 9-AOC enzyme activities. Using forward genetics via metabolite based association mapping in maize, efforts in the Schmelz laboratory identified a novel 9-AOC, termed Death Acid Synthase (DAS), and confirmed catalytic activity using *Agrobacterium*-mediated *Nicotiana benthamiana* heterologous enzyme expression assays with key combinations of established LOX, AOS

and 13-AOCs to generate appropriate substrates for comparisons. During my Masters thesis I used defined CRISPR/Cas9 maize *9-aoc* mutants to biochemically characterize plants for the endogenous loss of DA production, examine for non-target effects on maize antibiotic biosynthesis and explore alterations in disease resistance to fungal pathogens. Results support the existence of a single functional copy *9-aoc* in maize responsible for DA biosynthesis and additional biochemical immune layers that contribute to *Fusarium graminearum* resistance.

## **Introduction**

Plants colonize many different environments where they cope with a wide range of biotic and abiotic challenges. Evolution through time has provided them with a multitude of complex defense mechanisms. Many constitutive physical and chemical barriers prevent the establishment of most plant pathogens (War et al., 2012). When select pathogens overcome constitutive defenses, dynamic plant recognition mechanisms trigger a multitude of inducible defenses through the large scale transcriptional and proteomic reprogramming of the cells (Ding et al., 2020). Plants have a variety of inducible defenses in the presence of pathogens. In addition to specialized metabolites, plants produce antimicrobial proteins, such as chitinases and other lytic enzymes that can directly degrade pathogen cell walls and membranes. As part of the innate immune system, plants recognize microbe-associated molecular patterns (MAMPs) of potential pathogens through pattern recognition receptors (PRRs) that mediate a basal defense response. In turn, select plant pathogens can suppress inducible defense responses through the delivery of proteinaceous and small molecule effectors that effectively suppress or divert the defense response enabling disease (de Wit et al., 2007).

Plant diseases are most commonly caused by biotic stresses such as fungi, bacteria, and viruses; however, abiotic environmental factors such as nutrient deficiency, drought, hypoxia, temperature extremes, ultraviolet radiation, and heavy metal stress can also drive similar oxidative stress responses. In order to protect themselves from damage, plants rely on wide variety of constitutive and inducible defenses that partially overlap between during biotic and abiotic stress (Pelzcar et al., 2020).

To combat complex biotic stresses such as insect and pathogen attack, all plants rely on small-molecule specialized metabolites to serve as direct and indirect defenses (Dixon 2001). Present in all plants, terpenoids and phenylpropanoids are among the most structurally diverse classes of specialized metabolite pathways. Recently maize has been recognized to rely on diverse sesquiterpenoid and diterpenoid precursors for the production of non-volatile defenses and further roles in mediating responses to herbivores, pathogens, and other environmental challenges (Block et al., 2019). Following oxidation and conjugation, collectively terpenoids display massive structural diversity with over 80,000 compounds known in nature (Huang et al., 2019). Plant terpenoids play diverse roles including phytohormones, protection against UV light, serve as chemical barriers and mediating interactions between the plants and other surrounding organisms (Gershenzon and Dudareva, 2007). Phytoalexins constitute a broad category of pathogen- and insect-inducible biochemicals that locally protect plant tissues. Phytoalexins are classified as low-molecular-weight inducible specialized metabolites with activity against multiple biotic attackers. Terpenoids, including sesquiterpenes and diterpenes, constitute some of the commonly encountered chemical classes of phytoalexins in grain crops (Schmelz et al., 2014). Following insect attack, specific maize volatile terpenes serve as indirect defenses in both the roots and shoots (Turlings et al., 1990; Degenhardt, 2009; Degenhardt et al., 2009; Köllner et al., 2013). In contrast to insect attack, following fungal elicitation maize terpene olefins are less commonly detected volatiles and instead serve as precursors for the elicited accumulation of non-volatile terpenoids functioning as direct defenses limiting pathogen spread (Harborne, 1999; Ahuja et al., 2012; Ding et al., 2019).

The largest known family of maize antibiotics are the non-volatile acidic sesquiterpenoids, termed zealexins (ZXs) which are produced in response to fungal attack (Ding et al., 2020). The ZX family consists of least 17 precursors and products derived from a chromosome 10 gene cluster of 4 Terpene Synthases (TPS), termed Zx1 through Zx4, that encode  $\beta$ -bisabolene dependent  $\beta$ -macrocarpene synthases (Huffaker et al., 2011; Ding et al., 2020). A second ZX pathway gene cluster on Chromosome 5 contains three cytochrome P450 (CYP) genes in the CYP71Z family that encode the Zx5 (ZmCYP71Z19), Zx6 (ZmCYP71Z18) and Zx7 (ZmCYP71Z16) enzymes. Zx5, Zx6 and Zx7 collectively catalyze oxidation of  $\beta$ -bisabolene and  $\beta$ -macrocarpene to form  $\beta$ -bisabolene derived D-series and  $\beta$ -macrocarpene driven A-series zealexins (ZA1). Zx5 has also been shown to act on  $\alpha/\beta$ -selinene producing  $\alpha/\beta$ -costic acids (Ding et al., 2020). Similarly, Zx6 and Zx7 both share in catalyzing several oxidative steps in the dolabralexin (DX) and kauralexin (KX) diterpenoid defense pathways (Mafu et al., 2018; Ding et al., 2019).

Maize diterpenoid antibiotics are derived from *ent*-copalyl diphosphate synthase, termed anther ear 2 (ZmAN2), and the production of *ent*-copalyl diphosphate (*ent*-CPP). ZmAn2 derived *ent*-CPP is required for the kauralexin (KX) and dolabralexin (DX) production as both are missing in *Zman2* mutants (Christensen et al., 2018 and Mafu et al., 2018). The KX pathway further requires the type I diterpene synthase (DiTPS) termed Kaurene Synthase Like 2 (ZmKSL2) for the production of *ent*-isokaurene (Ding et al., 2019). Collectively oxidations and reductions by ZmCYP71Z18, ZmCYP71Z16, ZmCYP701A43 (ZmKO2) and Kauralexin Reductase 2 (KR2) commonly result in *ent*-kaur-19-al-17-oic acid (KA3) as a dominant antibiotic accumulating after fungal attack

(Ding et al., 2019). KX contribute to defense both above and below ground against pathogenic fungi such as *Fusarium* species. In response to stem attack by the European corn borer (*Ostrinia nubilalis*) the induced accumulation of KX are also observed and can function as feeding deterrents (Schmelz et al., 2011).

Similarly the DX pathway consists of the sequential activity of two diterpene synthases, ZmAN2 and Kaurene Synthase-Like4 (ZmKSL4) required for the production of the diterpene hydrocarbon dolabradiene. ZmCYP71Z18 and ZmCYP71Z16 can both produce 3 $\beta$ -epoxy-dolabranol is further converted into 3 $\beta$ ,15,16-trihydroxydolabrene (THD) (Mafu et. al., 2018). Epoxydolabranol is extremely potent as an antifungal agent and acts at 10 ug ml<sup>-1</sup> (Mafu et. al., 2018). Oxidative stress is shown to induce dolabralexin accumulation and transcript expression of *ZmAN2* and *ZmKSL4* in root tissues. Likewise, metabolite and transcript accumulation are up regulated in response to elicitation with the fungal pathogens *Fusarium verticillioides* and *F. graminearum* (Murphy et al., 2019).

Diverse arrays of plant specialized metabolites govern interactions with, and adaptation to, biotic and abiotic environments (Pichersky and Gershenzon, 2002; Hartmann, 2007; Pichersky and Lewinsohn, 2011; Tholl, 2015). Beyond terpenoids maize is know to contain a complex system of defense-related specialized metabolites, including phenylpropanoids, flavonoids, benzoxazinoids and oxylipins, (Santiago and Malvar, 2010; Ahmad et al., 2011; Christensen et al., 2015; Richter et al., 2016; Wouters et al., 2016). Recent advances in placing sesquiterpenoid antibiotic biosynthetic pathways in the context of additional layers of maize defenses demonstrate that over 1500 transcript-protein pairs are shared by the same regulatory module activated following

fungal elicitation (Ding et al., 2020). Given that less than 10% of the 1500 maize genes and encoded enzymes have been fully characterized, it is clear that our knowledge of biochemical defenses and pathway genes responsible for mitigating stresses on crops remain grossly incomplete.

Similar to maize terpenoids, diverse fatty acid derived oxylipins play a vital role in plant resistance against insect and pathogen attack as regulatory signals, direct defenses and indirect defenses (Borrego et al., 2016). One the most extensively studied examples is the linolenic acid (18:3)-derived pathway leading to the production of 12 carbon cyclopentanone molecule termed jasmonic acid (JA). JA and related jasmonates more broadly belong to a large group of oxygenated fatty acid derivatives termed oxylipins. Oxylipins are derived from either enzymatic or autoxidation of free or membrane-esterified fatty acids (Borrego et al., 2016). In plants, oxylipins are produced primarily from the enzymatic oxygenation of polyunsaturated fatty acids, linoleic (18:2) or linolenic acid (18:3) via lipoxygenase (LOX) enzymes with regiospecificity at the C9 and C13 positions or alpha-dioxygenase activity (Borrego et al., 2016). Upon plant damage, 9/13-lipoxygenases utilize fatty acid substrates to yield respective unstable 9- and 13-hydroperoxides. Linolenic acid is acted upon by 13-LOX enzymes, allene oxide synthases (AOS) to form an unstable epoxides and 13-allene oxide cyclases (13-AOC) to sequentially result in the production of 12-oxo-phytodienoic acid (12-OPDA) as an essential precursor to the production of jasmonates. (Borrego et al., 2016; Christensen et al., 2015). The reduction of a cyclopentenone ring by 12-oxo-phytodienoic acid reductase (OPR) and subsequent  $\beta$ -oxidation steps are then required to make 7-iso-JA (Christensen et al., 2015). Both jasmonic acid and 12-OPDA play many vital roles in plant physiology.

Following JA conjugation to isoleucine (Ile), JA-Ile binds to proteins, called JAZ and COI1, that then targets them to 26S-proteasome degradation and thus removes the negative regulation of transcription factors (such as MYC2) which can then activate plant defense responses (Shurtleff et al., 2020). Genes responsible for jasmonate biosynthesis and JAZ protein production represent the potential targets for genetic engineering in order to be able to produce plants with an increased resistance to disease (Shurtleff et al., 2020). This includes developmental processes and inducible defenses against biotic threats. In maize JA biosynthesis has been proven to play key roles in biotic stress survival, regulation of senescence, and cell death processes mediating male sex determination (Acosta et al., 2009, Yan et al., 2012, Christensen et al., 2015). The 12-OPDA signaling is in part mediated by TGA transcription factors which govern the detoxification responses such as cytochrome P450s (CYPs), glutathione S transferases and are consistent in a role with cell protection and survival.

Curiously in maize a conceptually similar JA-like pathway involves 9-LOX activity on linolenic and linoleic acid leads to the 12-OPDA positional isomer, 10-oxo-11-phytodienoic acid (10-OPDA) and 10-oxo-11-phytoenoic acid (10-OPEA) respectively. However the endogenous physiological roles for maize 9-LOX cyclopentenones and precise biosynthetic pathways have not yet been fully proven (Christensen et al., 2015). In developing maize leaves, an infection by southern leaf blight (SLB; *Cochliobolus heterostrophus*) results in necrotic tissue and the localized accumulation of 10-OPEA, 10-OPDA and a series of 14- and 12-carbon metabolites collectively termed Death Acids (DAs) (Christensen et al., 2015). Both 10-OPEA and 10-OPDA are broadly cytotoxic and following fungal elicitation and subsequent cellular

damage accumulate at high enough levels suppress the growth of fungi such as *Fusarium verticillioides*, *Aspergillus flavus* and corn earworm larvae (*Helicoverpa zea*) when examined *in vitro* (Christensen et al., 2015). In contrast to previously mentioned ZX and KX defenses, 10-OPEA and 10-OPDA display significant phytotoxicity in maize leaf assays (Christensen et al., 2015). A critical aspect of the current research is that no previously characterized 13-AOCs involved in JA biosynthesis are able to cyclize 9-AOS products. The production of death acids in maize represents an unusual example in nature where the confirmed synthesis of predominantly (9*S*,13*S*)-10-OPEA must be enzymatic and the result of an undiscovered novel 9-AOC acting on 9-LOX derived allene oxides (Ogorodnikova et al., 2015 and Christensen et al., 2015).

The goal of my Masters Thesis was to work towards the identification and characterization the maize 9-Allene Oxide Cyclase (9-AOC) enzyme, termed Death Acid Synthase (DAS), and to access the phenotypes of the maize CRISPR/CAS9 derived knock out *9-aoc/das* mutants to examine if production of DAs function as a direct defense against fungal pathogens. An important concept of this effort was to confirm that a single enzyme exists in maize and the defined *9-aoc* mutants lack pathogen inducible DAs. Likewise if DAs act as JA-like signals they could be compromised in other defense signaling pathways. For this reason we analyzed ZX, KX and DX metabolites in maize samples to consider if non-target pathways were impacted by the loss of pathogen inducible DA biosynthesis.

## **Materials and Methods**

### *Biological materials used*

Maize plants were grown in the greenhouses and fields at the UCSD Biology Field Station (BFS). For experiments involving maize scutella tissue in seedlings, all plants were grown in a walk-in plant growth chamber in Muir Biology (3<sup>rd</sup> floor). Goodman association panel seeds were obtained from the National Genetic Resources Program (GRIN; <https://www.ars-grin.gov/>) spanning 282 inbred lines. For forward genetic experiments, fungal elicited maize stems (3-5 day after treatments) were ground in liquid N<sub>2</sub> to a fine powder and stored at -80°C. Working with liquid N<sub>2</sub> and -80°C is essential to halt all enzyme activities and maintain stability of potentially labile analytes.

### **Chemical Analyses using Gas Chromatography/Mass Spectrometry (GC/MS)**

A simple approach to sample analysis relies on Vapor Phase Extraction (VPE) to remove high molecular weight analytes otherwise un-compatible with gas chromatography (GC). In this procedure 50 mg sample aliquots are weighed, extracted by organic solvent during vortexing/bead homogenization and the resulting organic phase is derivatized using trimethylsilyl diazomethane (Schmelz et al., 2004). VPE for a select number of samples were performed following Schmelz et al., (2004) using an Agilent 6890 series GC coupled to an Agilent 5973 mass selective detector (MSD) is described further below. Agilent Mass Hunter Qualitative and MS Quantitative Analysis software alongside Agilent ChemStation qualitative programs were used to generate and analyze the GC-MS generated chromatograms and spectra. Replicated experiments were

summarized with peak areas captured in MassHunter Qualitative Navigator B.08.00, and MS Quantitative Analysis B.08.00, quantified in Excel and statistically evaluated in JMP. MassHunter MS Quantitative program peak selection methods were manually produced taking into account retention time shifts. Program automated peak selections/integrations were instead substituted for manual selections/integrations of every target compound in every sample. This allowed for a much greater degree of accuracy in calculating compound concentrations and better overall genetic mapping.

### **A Modified and Improved Vapor Phase Extraction (VPE) Protocol**

To minimize artifact generation, biologic samples were frozen in liquid N<sub>2</sub> and maintained at -80°C immediately prior to solvent extraction. Samples were ground using a mortar and pestle and carefully transferred to 2 ml tubes. Tissue (50 mg) was placed into a 4 ml glass vial kept on liquid N<sub>2</sub>. For the routine analysis of diverse oxygenated plant terpenoids ALL handling steps including solvent pipetting, liquid handling, storage, and transfers requires glass syringes and glass vials. Immediately prior to extraction, finely ground samples in 4 ml glass vials are removed from the liquid N<sub>2</sub> and spiked with 500 µls of the extraction solvent, namely H<sub>2</sub>O: 1-propanol: HCl (1:2:0.005) with internal standards such as 400 ng heneicosanoic acid (21:0) following (Schmelz et al., 2004). A Teflon lined cap is then screwed on the vial and the sample is vortexed for 1 min and allowed to sit for 5 min. Next 1 ml of hexane is further added using a glass pipette tip, the vial is re-capped, briefly re-vortexed and allowed to settle for 10 min. The lower aqueous and upper hexane:1-propanol layers concentrate highly polar and lipophilic metabolites,

respectively. Use of internal standards quantitatively corrects for potential pH-derived differences in extraction efficiency between samples.

To increase volatility and improve gas phase chromatography of carboxylic acid containing analytes, the upper organic phase is transferred to a new clean 4-ml glass vial and derivatized directly using 7  $\mu$ l of trimethylsilyldiazomethane (2M in hexane)(Sigma-Aldrich) to generate to methyl esters following gentle shaking and a 15 min reaction time. Unlike previous VPE protocols (Schmelz et al., 2004) excess trimethylsilyldiazomethane is not neutralized excess excess trimethylsilyldiazomethane are removed under a N<sub>2</sub> stream to dryness. For analyses seeking to include volatile analytes, such as sesquiterpene and diterpene hydrocarbon olefins, the sample must not be over-dried.

The volatile collection filters, termed VPE traps, are constructed from inert materials including glass, fluorocarbons, and stainless-steel/nylon mesh (Schmelz et al., 2004). The adsorbent present in VPE traps is Porapak Q (80-100  $\mu$ m mesh termed Super Q) (Sigma Aldrich), a divinylbenzene polymer tolerant most solvents and sensitive only to temperatures above 300°C or the presence of strong acids. To make use of Porapak Q properties and increase the range of analytes recovered, volatilization temperatures of 200°C were used (Schmelz et al., 2004). Sample collection procedure is as follows: (i) N<sub>2</sub> stream through the needle is initiated with surplus pressure released to a bubbler with the existing flow exceeding the vacuum once the system is fully linked. (ii) A 500 ml min<sup>-1</sup> flow is generated by chemically resistant teflon-membrane vacuum pump calibrated with a needle valve and periodically confirmed using a flowmeter. (iii) The VPE trap is first inserted into the high temperature septa, followed by the N<sub>2</sub> stream needle, and finally the

vacuum line is connected to the VPE trap. Upon proper connection, solvent vapors pass through the VPE trap and the collection of volatile analytes is initiated. At this time, the dry vial is transferred to a heating block at 200°C for 2 min. Once the VPE collection process is completed, the sample is disassembled by handling the vacuum and N<sub>2</sub> supply lines and open top caps, with care taken to avoid touching the heated glass. For analysis, the VPE trap are eluted into a GC/MS sample vial with 200 µl of ethyl acetate: hexane (1:1) and analyzed by GC/MS. Specifically for tobacco (*Nicotiana benthamiana*) metabolite analyses, prior to the extraction described above, tissue aliquots were subjected to β-glucosidase treatment (Sigma-Aldrich, Co, LLC, USA) in 250 µl 0.1 M sodium acetate buffer (pH=5.5) at a concentration of 100 units ml<sup>-1</sup> at 37°C for 30 minutes before solvent extraction.

### **Gas chromatography/mass spectrometry (GC/MS) analyses of metabolites**

GC/MS analysis utilized an Agilent 6890 series gas chromatograph (GC) joined to an Agilent 5973 mass selective detector (MS-D; mass temperature, 150 °C; interface temperature, 250 °C; electron energy, 70 eV; source temperature, 230°C). A DB-35 MS column (Agilent; 30 m × 250 µm × 0.25 µm film) was used for gas chromatography. Samples were introduced, with an initial oven temperature of 45 °C, as a splitless injection. The temperature was held for 2.25 min, then increased to 300 °C with a gradient of 20 °C min<sup>-1</sup> and held at 300 °C for 5 min. A solvent delay of 4.5 min was selected to prevent ethyl acetate present in the sample from damaging the electron ionization (EI)-filament. GC/MS analyses and diagnostic EI spectra of ZX, KX, DX and DA metabolites follow from previous efforts (Christensen et al.,

## **Forward Genetic Mapping to Uncover Potential DA Gene Candidates**

In order to find metabolite variation in the levels of fungal-elicited 10-OPEA that accumulate in maize stems, diverse inbred lines were examined from the Nested Association Mapping (NAM) collection (McMullen et al (26)). From this early screen, the B73 x CML247 subpopulation of recombinant inbred lines (RILs) and the Goodman diversity panel (Flint-Garcia et al. 2005) were selected. Elicitation of maize stem tissues with heat-kill fungal hyphae for 3 days was performed as was previously described for the GWAS and RIL studies respectively (Ding et al., 2019). Genotypic data for the NAM B73 × CML247 RIL subpopulation (NAM imputed AllZea GBS Build July 2012 FINAL, AGPv2) and Goodman Diversity panel (Maize HapMapV3.2.1 genotypes with imputation, AGPv3) were downloaded ([www.panzea.org](http://www.panzea.org)). SNPs with less than 20% missing genotype data and minor allele frequencies > 5% were employed in the association analysis resulting in the final use of 80,440 SNPs and 25,457,708 SNPs for the RIL and diversity panel, respectively. For the NAM B73 × CML247 RILs, composite interval mapping implemented in Windows QTL. Cartographer.v2.5 (<https://brcwebportal.cos.ncsu.edu/qtlcart/WQTLCart.htm>) following Ding et al., (2019).. Analyses of the GWAS for the Goodman association panel were initially conducted in TASSEL 5.0 using the Mixed Linear Model (MLM). Manhattan plots were generated in TASSEL and RStudio.

## **Phylogenetic and Expression Analysis of the Maize Germin-Like Family Genes**

With the help of Dr. Ding, a maximum likelihood phylogenetic tree of amino acid sequences annotated as germin-like family proteins in the B73 genome (RefGen\_V3) was constructed using Mega 7.0. A phylogenetic tree of the different amino acid sequences of the B73 germin family were created in order to compare the SLB elicited leaf expression of our top gene candidate *GRMZM2G090245* to all other members of the maize GLP family. RNAseq raw data (GSE120135 from <http://www.ncbi.nlm.nih.gov/geo/>) were re-analyzed based on the B73 RefGen\_V3 to obtain transcriptome data for SLB elicited leaves.

## **Transient enzyme co-expression assays in tobacco (*Nicotiana benthamiana*)**

With the significant efforts of Dr. Ding, combinatorial *Agrobacterium*-mediated heterologous enzyme expression assays were conducted in tobacco (*N. benthamiana*) using combinations of maize LOX and AOS to generate appropriate substrates for 13-AOC and 9-AOC activity comparisons. In order to understand both the established maize jasmonic acid pathway and the unproven DA pathway, the previously characterized maize enzyme LOX8 was selected. *E. coli* expressed LOX8 displays a 1:1 production of both 9- and 13-hydroperoxides and is endogenously required for JA production in maize pistal primordia (Acosta et al., 2009). We made use of dual specificity of maize LOX8 and paired it with the predicted allene oxide synthase AOS3 (GRMZM2G376661) (Borrego and Kolomiets 2016). While the specific genes expressed differ, basic procedures surrounding the *Agrobacterium*-based delivery of transient heterologous

expression constructs to *N. benthamiana* follow from Ding et al. (2019; 2020). Five days post *Agrobacterium* leaf infiltration *N. benthamiana* leaf tissue was harvested, ground to a fine powder in N<sub>2</sub> and saved for enzyme assays using 18:2 and 18:3 as substrates following by methylation and analysis. Samples were then analyzed as extracted ion chromatograms (EIC). To focus on a few reasonable maize AOS pathway candidates, maize transcriptomic data sets were used following stem elicitation with fungus. Two maize AOS (GRMZM2G067225 and GRMZM2G376661) were ultimately chosen for expression analysis.

#### **Source of *9-aoc* maize mutants**

Dr. Bing Yang (Danforth Center), Dr. Yezhang Ding and Mengxi Wu, performed a collaborative joint effort in collectively generating maize *9-aoc* knock out (KO) mutants in the B73 inbred line. The single maize *9-AOC* gene was targeted for precise mutations using clustered regularly interspaced short palindromic repeat (CRISPR)-associated protein 9 (Cas9) genome editing approaches (CRISPR/Cas9) following (Char and Yang, 2020). The first characterized *9-aoc* mutation results from a 4 nucleotide (NT) deletion and a 1 NT insertion that causes a single amino acid deletion followed by 10 non-synonymous AA changes near N-terminal which are then recovered back to the wild type AA sequence for the remainder of the protein. The second isolated mutation begins in a similar position near the N-terminal but resulted in 95% of the entire protein having non-synonymous AA changes. Dr. Yezhang Ding and Mengxi Wu performed extensive genotyping of segregating seeds, selection of lines, maize propagation, outcrossing, selfing and collection of final maize seeds used in this effort.

### **Analysis of *9-aoc* mutants deficient in DA production in from maize scutella tissue**

The subterranean scutella tissue of young maize seedlings gradually increases in 10-OPEA over time in a process coincident with increasing level of cell death (Christensen et al., 2016). Wild type (WT) B73 and *9-aoc* mutant maize seeds (n=4) were successively planted 4 days apart and all plants were harvested on the same day allowing ages of 9, 13, 17, 21 and 25 day old to be uniformly harvested. Scutella were carefully separated to remove remaining endosperm, pericarp, mesocotyl and root tissues. The scutella were then ground in liquid N<sub>2</sub> in, transferred to a 2 ml tube, and stored in -80°C freezer to halt enzymatic activity until ready for vapor phase extraction (VPE) (Schmelz et al., 2004). Samples were then processed for metabolite analysis as described previously.

### **Analysis of endogenous DA production in maize *9-aoc* mutants following fungal challenge**

In order to examine local DA production, 2 different of CRISPR/Cas9 derived *9-aoc* mutants were analyzed for stem defenses following fungal challenge with SLB and *F. graminearum*. Specifically maize stems were inoculated with either *Fusarium graminearum* (Fg.) or southern leaf blight (SLB; *Cochliobolus heterostrophus*) spores at 34 days old and harvested 8 days later at 42 day old. The basal node tissue of the 34 day old plants were punctured with an 18 gage needle, inoculated with spores (10 µl of 1 x 10<sup>5</sup> spores ml<sup>-1</sup>) and sealed with tape in order to prevent desiccation for the 8 day

experiment. Both fungal-infected tissues (local, 1 cm on either side of the inoculation site) and adjacent tissues (distal, 2 cm from the site of visible necrosis) were analyzed in B73 WT and *9-aoc* mutants. Samples were then carefully ground in liquid N<sub>2</sub> in powdered form, transferred to a 2 ml tube, and stored in -80°C freezer to halt enzymatic activity until ready for vapor phase extraction (VPE) (Schmelz et al., 2004).

## Results

### **Multiple forward genetics approaches support a shared locus on chromosome 6 associated with 10-OPEA levels following fungal elicitation of maize stems**

Maize DA biosynthesis is consistent with the presence of a novel 9-AOC activity (Christensen et al., 2015). Following previous efforts to understand fungal-elicited defenses in maize stems (Ding et al., 2019), a Genome Wide Association Study (GWAS) was conducted with the Goodman diversity panel (Flint-Garcia et al., 2005) and the Nested Association Mapping (NAM) B73 x CML247 recombinant inbred line (RIL) sub-population using 10-OPEA levels as phenotypic trait. Elicitation of maize stem tissues with heat-kill fungal hyphae for 3 to 5 days was previously described for the GWAS and RIL studies, respectively (Ding et al., 2019). 10-OPEA levels were measured by GC/MS. Metabolite lead GWAS identified statistically significant single nucleotide polymorphisms SNPs on Chr. 6 near position 161,200,000 (B73 RefGen\_V3) (Fig. 1) in a region spanning approximately 70 genes. Linkage Analysis using the B73 x CML247 recombinant inbred line (RIL) sub-population further revealed a shared statistically significant Quantitative Trait Locus (QTL) on chromosome 6 spanning the same region (160-163 Mb) (Fig. 1). Changes in maize leaf transcript accumulation following SLB infection of maize leaves was used as an initial filter to narrow the selection of candidate genes (Ding et al., 2019). In this dataset spanning the GWAS mapping interval a single gene was identified that had an extremely large fold increase following elicitation ( $>5000$  log<sub>2</sub>) (Table 1). The top candidate gene was *GRMZM2G090245* which is annotated as a germin-like protein / Cupin domain containing protein. Maize germin-like proteins (GLP) are predicted to encoded representing a medium sized gene family with 45 members. Dr.

Yezhang Ding then created a phylogenetic tree of the different amino acid sequences of the B73 germin family. The SLB elicited leaf expression of *GRMZM2G090245* was then compared all other members of the maize GLP family and found to be the highest by a factor of 10 (Fig. 2). From the mapping results and gene family analyses we hypothesized that of all encoded maize GLP in the B73 genome, *GRMZM2G090245* could be a predominant interacting protein involved in DA biosynthesis during pathogen attack.

### **Heterologous expression of select candidate DA biosynthetic proteins in tobacco to support 9-allene oxide cyclase (9-AOC) activity.**

With conceptual similarities to the jasmonate biosynthetic pathway, DA biosynthesis is predicted to require 9-LOX activity on linoleic acid (18:2) and linolenic acid (18:3) following by the conversion of 9-hydroperoxides to unstable epoxides via allene oxide synthase (9/13-AOS), and finally cyclization by 9-allene oxide cyclase (9-AOC) to form 10-OPDA/10-OPEA (Christensen et. al., 2015). Maize contains 13 different *LOX* genes and 5 *AOS* genes, with differing product specificities but none that are 100% 13-LOX or 9-LOX (13-AOS/9-AOS) but instead have differing proportions of regiospecificity at the 9 and 13 positions (Borrego and Kolomiets, 2016). To understand both the established maize JA pathway and the yet unproven DA pathway we selected the previously characterized maize enzyme LOX8 which displays a 1:1 production of both 9- and 13-hydroperoxides and is required for JA production in maize pistal primordia (Acosta et al., 2009). Transcriptomic datasets following stem elicitation with fungus supported multiple AOS candidates to consider however 2 were finally were selected for expression analysis [*GRMZM2G067225*; AOS1 (AOS2b) & *GRMZM2G376661*; AOS3

(AOS1a)]. To our knowledge GRMZM2G376661 / AOS3 had not been biochemically characterized before. Maize 13-allene oxide cyclase (13-AOC) activity has been characterized and has 2 predicted 13-AOC genes based on homology to established Arabidopsis homologs (Borrego and Kolomiets, 2016). We selected the gene *GRMZM2G077316* (*AOC1*) as a candidate 13-AOC and positive control for 12-OPDA biosynthesis. Combinatorial *Agrobacterium*-mediated heterologous enzyme expression assays were then conducted in tobacco (*N. benthamiana*) with using maize LOX and AOS to generate appropriate substrates for 13-AOC and 9-AOC activity comparisons. 5 days after *Agrobacterium* leaf infiltration. *N. benthamiana* leaf tissue was harvested, ground to a fine powder in N<sub>2</sub> and saved for enzyme assays using 18:2 and 18:3 as substrates following by methylation and analysis. Analyzed as extracted ion chromatograms (EIC), we detected the statistically significant and selective formation of 10-OPEA following the co-expression maize LOX8, AOS3 and the novel 9-AOC following 18:2 substrate feeding (Fig 3a). With nearly identical results, co-expression of maize LOX8, AOS3 and the 9-AOC with 18:3 substrate yielded 10-OPDA. The JA pathway precursor 12-OPDA was likewise selectively produced in the presence of LOX8, AOS3 and AOC1 (13-AOC). Low levels of the 18:2 derived cyclopentenone, 15,16-dihydro-12-oxo-phytodienoic acid, occurred as a uniform background in all samples using 18:2 as a substrate thus providing a marker for a related yet non-specific metabolite. Using LOX8 as a known dual 1:1 regiospecific 9/13-LOX and AOS3 as a representative 9/13-AOS our results support AOC1 (13-AOC) and the novel non-canonical 9-AOC as selective and specific branch points in the in biosynthesis of jasmonate precursors and DAs.

## **A Maize *9-aoc* Mutant Selectively Lacks Endogenous DAs Defenses In Scutella**

### **Tissue**

Dr. Bing Yang (Danforth Center), Dr. Yezhang Ding and Mengxi Wu collectively generated targeted CRISPR/Cas9 mutants to create the maize *9-aoc* knock outs (KOs) in the B73 inbred line. Ultimately 2 different types of *9-aoc* KO mutants could be recovered. The first comparatively small *9-aoc* mutation resulting 4 nucleotide (NT) deletion and a 1 NT insertion causing a single amino acid deletion followed by 10 non-synonymous AA changes near N-terminal which are then recovered back to the wild type AA sequence for the remainder of the protein. The second mutation is begins similar position near the N-terminal similar yet results in 95% of the entire protein having non-synonymous AA changes. To first confirm that even modest mutations in the 9-AOC result in loss of DA production, I examined a time course of metabolites in maize scutella tissue post germination in soil where the DA is known become highly expressed over time (Christensen et al., 2016). Post germination scutella were examined from B73 wild type (WT) and the 11AA *9-aoc* mutation (g198) 9, 13, 17, 21 and 25 days after planting. We used zealexin (ZX), kauralexin (KX), and dolabralalexin (DX) pathway metabolites as additional lipid defense markers that should be unlinked based on different biosynthetic pathways. Overall no major differences in metabolite abundance trends were observed for ZX, KX and DX metabolites when comparing WT B73 scutella and the *9-aoc* mutant (Fig. 4). At the final 25 day time point, no evidence could be found for biosynthetic impairment of terpenoid defenses in the *9-aoc* mutant. As predicted from earlier studies (Christensen et al., 2016) levels of both 10-OPEA and 10-OPDA significantly increase over time in the B73 scutella (Fig. 5). In contrast, 10-OPEA and 10-OPDA levels remain

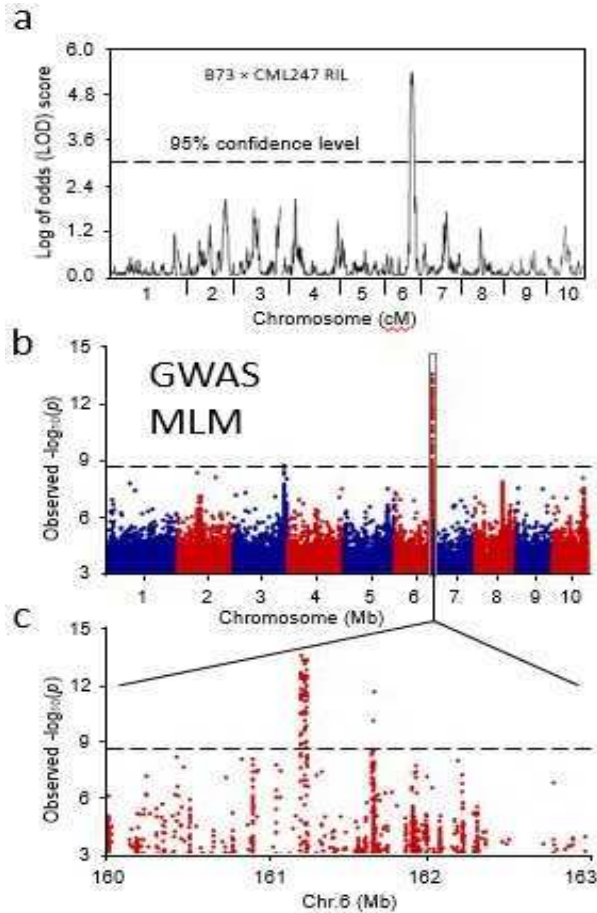
undetectable in the *9-aoc* mutant over all measured time points (Fig. 5). Collectively these results that even modest AA changes result in an endogenous null *9-aoc* mutation that selectively targets DA production and not other acidic lipid defenses.

**Maize *9-aoc* mutants lack DA production in stems following challenge with the stalk rotting fungus *Fusarium graminearum*.**

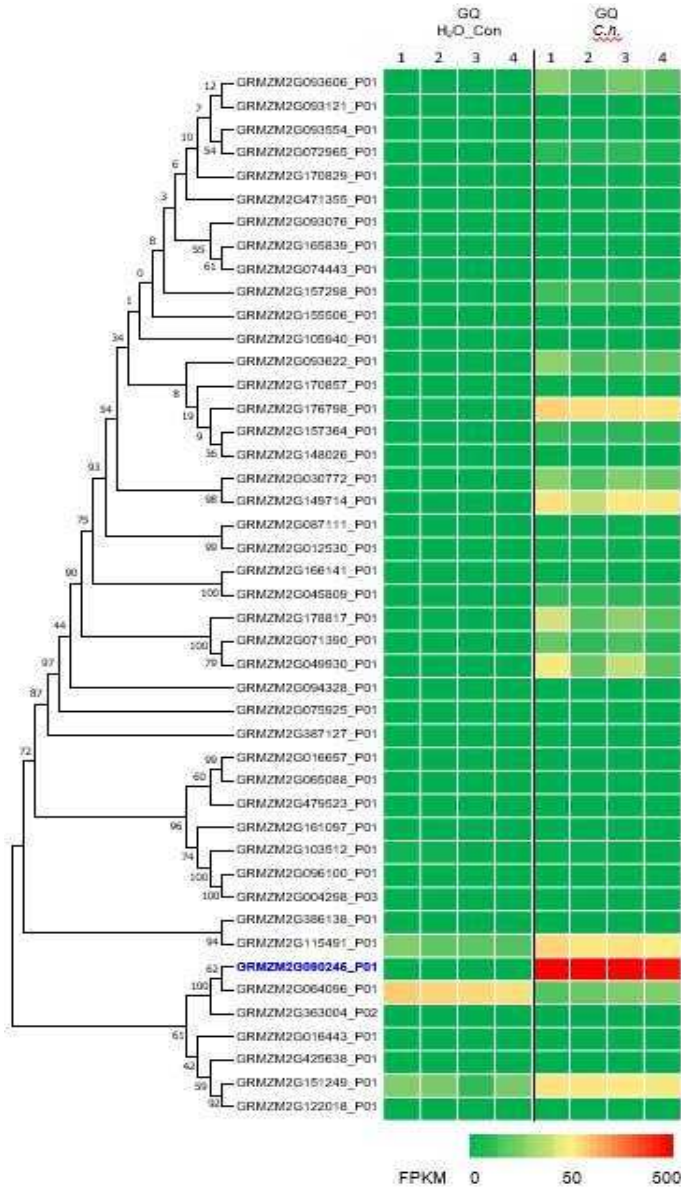
In growing maize seedlings, oil-rich scutella tissues below ground undergo programmed senescence in a microbe rich environment. For a more controlled experiment, we selected maize stem tissues for additional bioassays. I examined the 2 types of CRISPR/Cas9 derived *9-aoc* mutants in rapidly growing stem tissues following fungal challenge with SLB and *F. graminearum*. Basal node tissue of 42 day old plants was punctured with an 18 gage needle, inoculated with spores (10  $\mu$ l of  $1 \times 10^5$  spores ml<sup>-1</sup>), sealed with tape to prevent desiccation for the 8 day experiment. In response to both fungal pathogens, WT B73 plants accumulated significantly higher levels of both 10-OPEA (Fig. 6a) and 10-OPDA (Fig. 6b) in locally infected tissues compared to the 2 different *9-aoc* mutants (g198 and g274) with statistically significantly lower levels in the two mutant lines. Distal tissues of WT plants had significantly lower levels of 10-OPDA consistent with previous observations of DA as highly localized defenses. Collectively both types of CRISPR/Cas9 derived *9-aoc* mutants result in a loss of endogenous DA production in maize.

## **Maize *9-aoc* mutants are not compromised in the production zealexin antibiotics**

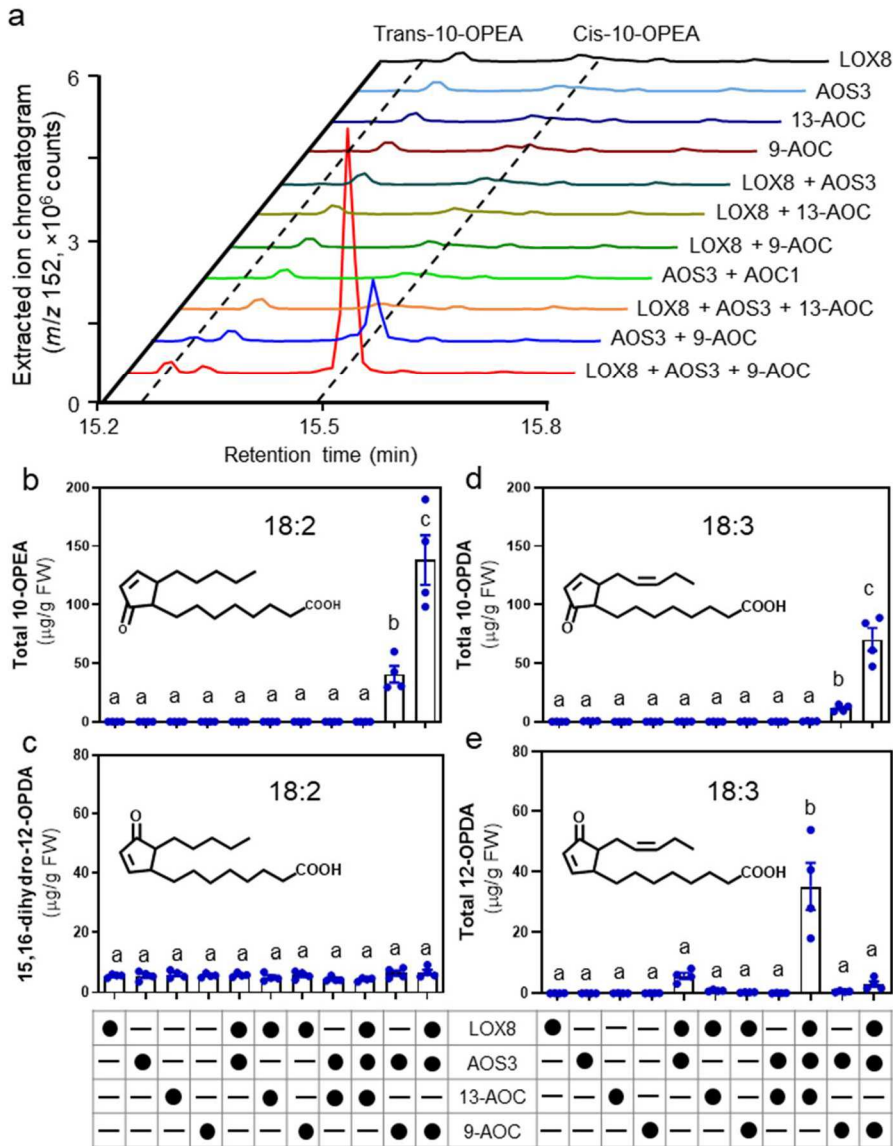
I further wanted to consider zealexin levels as second pathway and defense marker in the maize *9-aoc* mutants. Following from the previously described experiment, stem tissues were inoculated with either *Fusarium graminearum* (Fg.) or *southern leaf blight* (SLB; *Cochliobolus heterostrophus*). Unlike deficient levels of DAs, the *9-aoc* mutants accumulated high levels of zealexins metabolites such as ZA1, ZA2, ZA6, ZB1, ZC1 and ZD1 (Fig. 7). Interestingly, there was a statistically significant increase total ZX accumulation in the g274 *9-aoc* mutant compared to the wild type B73 stems following infection with both fungal species (Fig. 7). These results are consistent 2 hypotheses. Firstly, the *9-aoc* mutant is selectively impaired in DA biosynthesis. Secondly, *9-aoc* mutants can have greater levels of diseased tissue as indicated by the comparatively elevated zealexin levels.



**Figure 1. Combined linkage and association mapping identifies a locus on Chr.6 for total 10-OPEA content.** **a**, Linkage analysis of total 10-OPEA content in the B73 × CML247 recombinant inbred line mapping population. 10-OPEA was quantified with GC-MS from 5-d fungal elicited stems. cM, Centimorgan. **b**, Manhattan plot of the association analysis (MLM) of total 10-OPEA content in the stems of Goodman diversity panel following 3 d of fungal elicitation. The dashed line denotes the 5% Bonferroni corrected threshold for 25,457,708 SNP markers, with the most statistically significant SNP located at position 161,215,288 (B73 RefGen\_v3) on Chr.6. **c**, A regional Manhattan plot representing a 'zoomed-in' view of the signal between 160 Mb and 163 Mb on Chr.6, and each dot representing a single SNP.



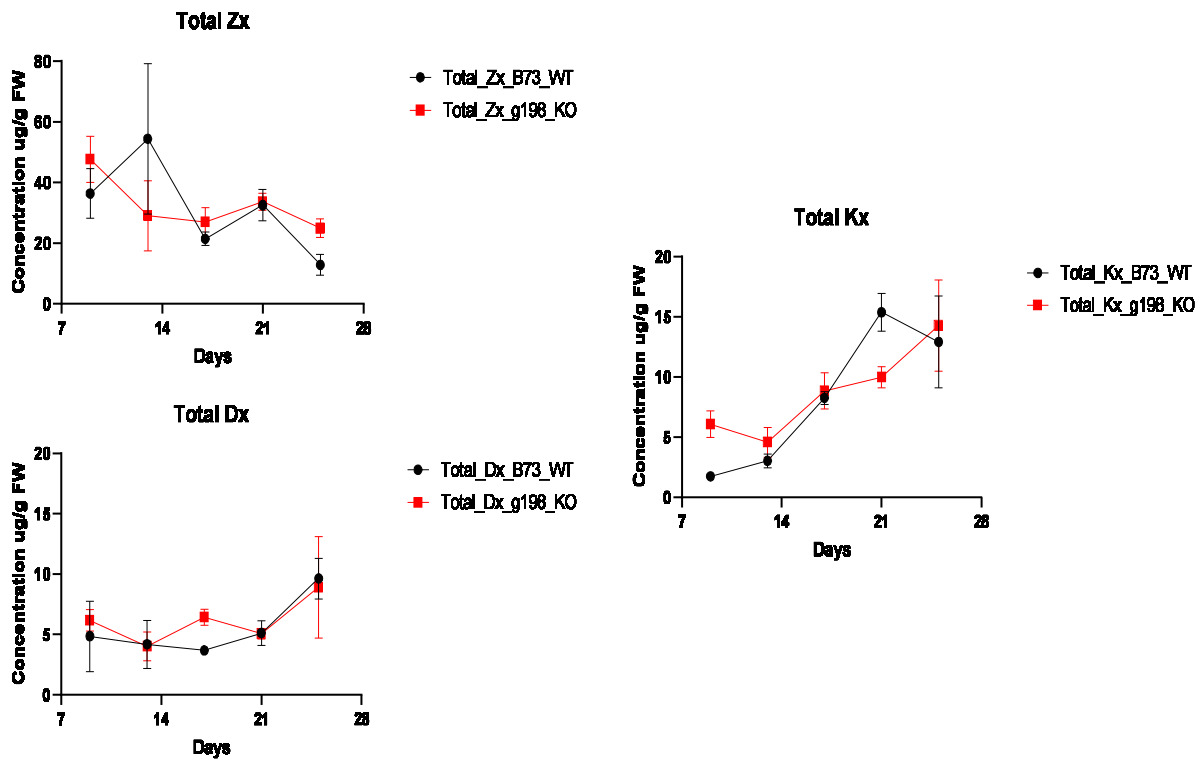
**Figure 2. Phylogenetic and expression analysis of the maize germin-like family genes.** Maximum likelihood phylogenetic tree of amino acid sequences annotated as germin-like family proteins in the B73 genome (RefGen V3) was constructed using Mega 7.0. Bootstrap values calculated from 1000 iterations are indicated at the nodes. The expression of each germin-like gene represented as the fragments per kilobase of transcript per million mapped reads (FPKM). The RNAseq raw data (GSE12013 from <http://www.ncbi.nlm.nih.gov/geo/>) were re-analyzed based on the B73 RefGen V3).



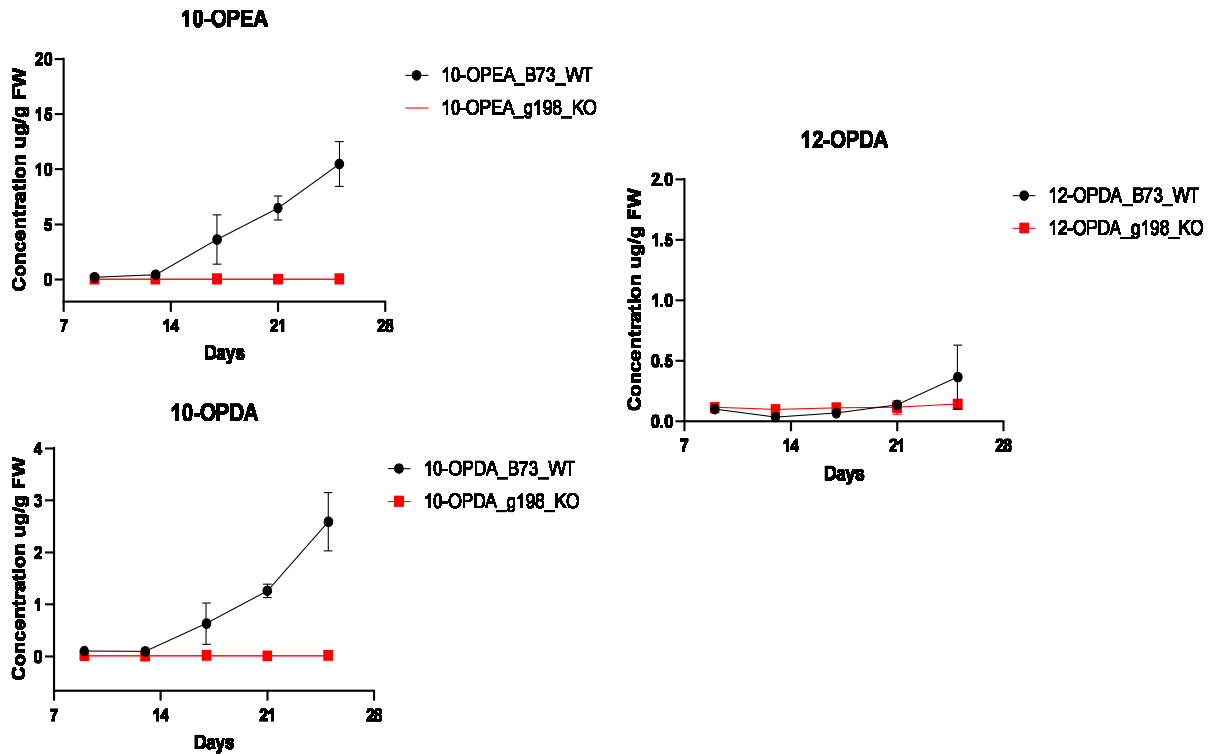
**Figure 3. A maize germin-like protein (GLP) functions as a 9-AOC for Death Acid biosynthesis.** **a**, Extracted ion chromatogram (EIC) exhibiting the formation of 10-OPEA through co-expressing the candidate 9-AOC with the maize LOX8 and AOS3 in *N. benthamiana* followed by 18:2 substrate feeding, as compared to a maize 13-AOC (AOC1) showing no activity in the death acid biosynthesis. Production of **b** (total 10-OPEA), **c** (15,16-dihydro-12-oxo-phytodienoic acid), **d** (total 10-OPDA), and **e** (total 12-OPDA) through transient expression of the different construct combinations in *N. benthamiana* followed by feeding 18:2 or 18:3 as indicated. Black circle representing presence and minus representing absence. Error bars in **b**, **c**, **d** and **e** indicate mean  $\pm$  s.e.m. ( $n = 4$  biologically independent replicates). Within plots, different letters (a–c) represent significant differences (one-way ANOVA followed by Tukey’s test corrections for multiple comparisons,  $P < 0.05$ ).

Table 1: GWAS mapping interval identified using 10-OPEA levels as a metabolic trait in the Goodman association panel and SLB-elicited leaf transcript levels (24h post inoculation) as a filter in the consideration of gene candidates. RNA-seq data was previously used in the description of kauralexin biosynthetic pathway genes (GSE120135 from <http://www.ncbi.nlm.nih.gov/geo/>) See: Ding Y, Murphy KM, Poretsky E, Mafu S, Yang B, Char SN, Christensen SA, Saldivar E, Wu M, Wang Q, et al. Multiple genes recruited from hormone pathways partition maize diterpenoid defences. Nat. Plants 2019, 5:1043-1056

Gene ID (RefGen_V3)	V3 Chr om.	v3_start	v3_end	Log2 Fold change (SLB 24h/Con 24h)
GRMZM2G094935	Chr6	161060698.0	161065860.0	4.5
GRMZM2G334658	Chr6	161205980.0	161206405.0	1.0
GRMZM2G035430	Chr6	161207412.0	161213186.0	3.5
GRMZM2G126048	Chr6	161225808.0	161233289.0	0.9
GRMZM2G126079	Chr6	161249612.0	161256814.0	89.8
GRMZM2G310739	Chr6	161307075.0	161311900.0	1.0
GRMZM2G014303	Chr6	161321890.0	161325363.0	1.3
GRMZM2G310758	Chr6	161325742.0	161328172.0	6.1
GRMZM2G014458	Chr6	161329314.0	161331455.0	0.9
GRMZM2G329776	Chr6	161360705.0	161363956.0	1.0
GRMZM2G158901	Chr6	161409589.0	161413628.0	2.2
GRMZM2G158972	Chr6	161413800.0	161420255.0	3.6
GRMZM2G159008	Chr6	161421079.0	161424892.0	0.4
GRMZM2G159032	Chr6	161426908.0	161429635.0	6.1
GRMZM2G159404	Chr6	161437417.0	161439254.0	0.7
GRMZM2G460542	Chr6	161440931.0	161443974.0	1.0
GRMZM2G034225	Chr6	161475410.0	161479568.0	0.9
GRMZM2G546254	Chr6	161543914.0	161548356.0	0.5
GRMZM2G406674	Chr6	161605699.0	161611370.0	5.1
GRMZM2G106607	Chr6	161611326.0	161614853.0	1.0
GRMZM2G115049	Chr6	161642062.0	161645447.0	4.2
GRMZM2G090245	Chr6	161647240.0	161648156.0	6626
GRMZM2G090087	Chr6	161650053.0	161657588.0	7.4
GRMZM2G090034	Chr6	161659661.0	161661428.0	1.3
GRMZM5G863420	Chr6	161673003.0	161674439.0	4.4
GRMZM2G445423	Chr6	161679196.0	161682228.0	3.9
GRMZM2G476843	Chr6	161738905.0	161743761.0	2.0
GRMZM2G177386	Chr6	161744096.0	161747484.0	3.7
GRMZM2G164676	Chr6	161750718.0	161815082.0	1.4
GRMZM2G016503	Chr6	161833045.0	161846216.0	1.1
GRMZM2G111017	Chr6	161851517.0	161854538.0	0.2
GRMZM2G121186	Chr6	161855885.0	161859125.0	5.2
GRMZM2G121208	Chr6	161903231.0	161906492.0	3.3
GRMZM2G121229	Chr6	161907862.0	161911092.0	2.5
GRMZM2G121237	Chr6	161911254.0	161915727.0	27.6
GRMZM2G121262	Chr6	161916081.0	161920668.0	4.8
GRMZM2G074790	Chr6	161921394.0	161927125.0	10.6
GRMZM5G899656	Chr6	161989300.0	161990563.0	12.8
GRMZM2G088995	Chr6	161992902.0	161993848.0	1.6
GRMZM5G847982	Chr6	161998678.0	162000549.0	0.3



**Figure 4: Maize terpenoid production is not inhibited in *9-aoc* single mutant *g-198*.** Average (n=4, ± SEM) Zealexin (Zx), Dolabralalexin (Dx), and Kauralexin (Kx) concentrations ( $\mu\text{g g FW}^{-1}$ ) in 25 day old maize scutella. Time course experiment was done over a 25-day period. *9-aoc-g198* display different amino acid changes in the CRISPR/Cas9 targeted 9-AOC.



**Figure 5: Maize *9-aoc* mutant lacks accumulation of Death Acids in mature B73 scutella.** Average ( $n=4$ ,  $\pm$  SEM) 10-OPEA, 10-OPDA, 12-OPDA concentrations ( $\mu\text{g g FW}^{-1}$ ) in 25 day old maize scutella. Time course experiment was done over a 25-day period. *9-aoc-g198* display different amino acid changes in the CRISPR/Cas9 targeted *9-AOC*.

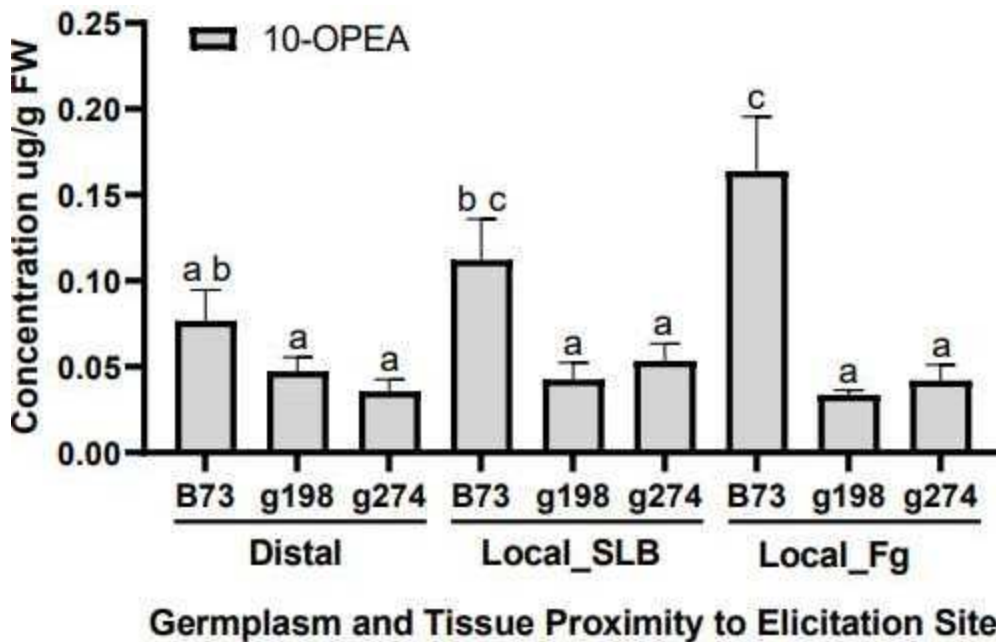


**Figure 6a: Maize 9-aoc mutants lack fungal elicited production of the linoleic acid (18:2) derived death acid 10-oxo-11-phytoenoic acid (10-OPEA).** Average (n=4, ± SEM) 10-OPEA concentrations (µg g FW<sup>-1</sup>) in 42 day old maize stems 8 days after inoculation with either *Fusarium graminearum* (*F.g.*) or southern leaf blight (SLB; *Cochliobolus heterostrophus*). 9-aoc-g198 and 9-aoc-g274 mutants display different amino acid changes in the CRISPR/Cas9 targeted 9-AOC. Local tissues included 2 cm of stem immediately surrounding the infection site. Distal stem tissues were 10 cm away and displayed no visual disease symptoms. Different letters (a–c) represent significant differences. Statistical analysis was performed using one-way ANOVA ( $P < 0.05$ ; Tukey tests were used to correct for multiple comparisons;  $P < 0.05$ ).

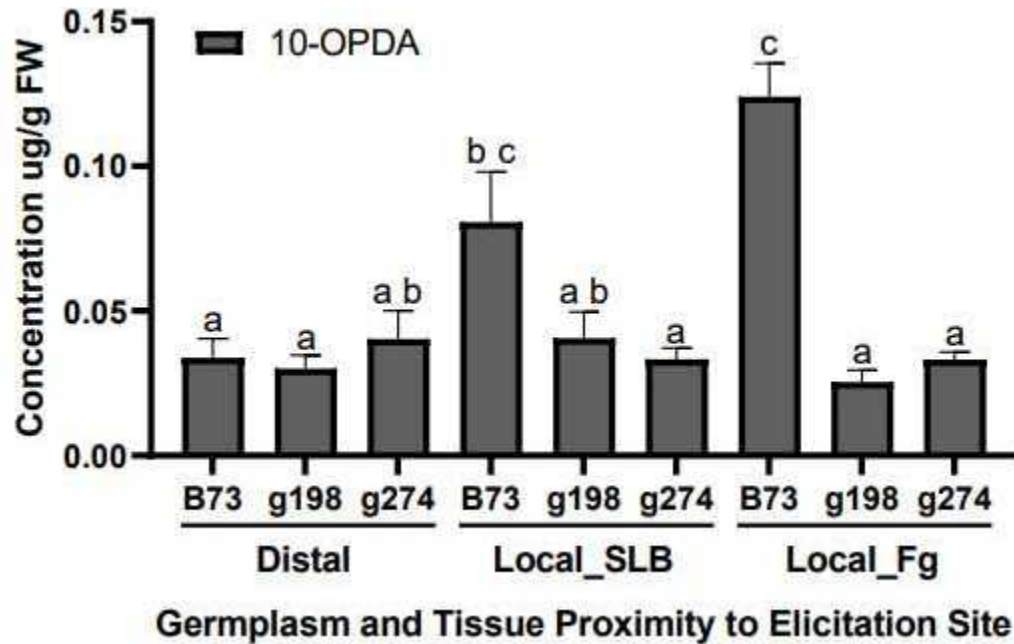


**Figure 6b: Maize *9-aoc* mutants lack fungal elicited production of the linolenic acid (18:3) derived death acid, 10-oxo-11-phytodienoic acid (10-OPDA).** Average ( $n=4$ ,  $\pm$  SEM) 10-OPDA concentrations ( $\mu\text{g g FW}^{-1}$ ) in 42 day old maize stems 8 days after inoculation with either *Fusarium graminearum* (*F.g.*) or southern leaf blight (SLB; *Cochliobolus heterostrophus*). *9-aoc-g198* and *9-aoc-g274* mutants display different amino acid changes in the CRISPR/Cas9 targeted 9-AOC. Local tissues included 2 cm of stem immediately surrounding the infection site. Distal stem tissues were 10 cm away and displayed no visual disease symptoms. Different letters (a–c) represent significant differences. Statistical analysis was performed using one-way ANOVA ( $P < 0.05$ ; Tukey tests were used to correct for multiple comparisons;  $P < 0.05$ ).

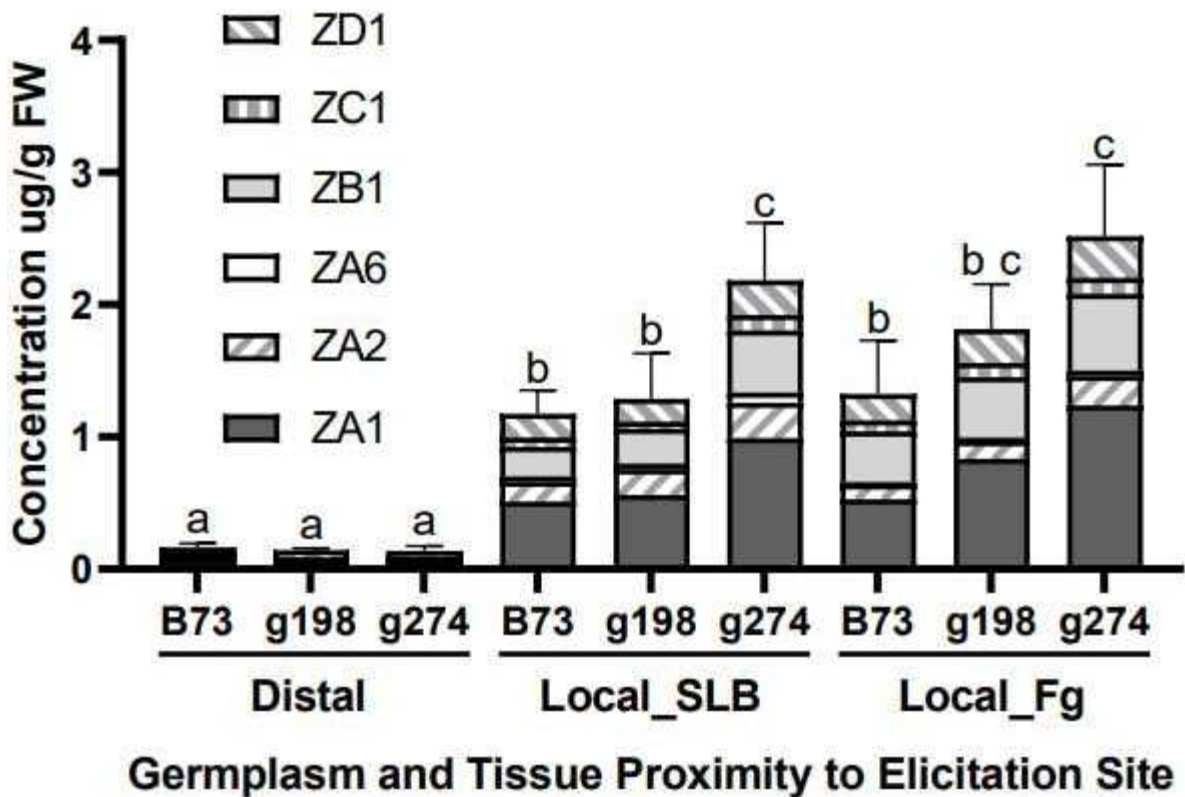


**Figure 7: Maize *9-aoc* mutants are not compromised in fungal elicited zealexin antibiotic production.** Average total (n=4,  $\pm$  SEM) zealexin concentrations ( $\mu\text{g g FW}^{-1}$ ) (sum of ZA1, ZA2, ZA6, ZB1, ZC1, ZD1) in 42 day old maize stems 8 days after inoculation with either *Fusarium graminearum* (Fg) or southern leaf blight (SLB; *Cochliobolus heterostrophus*). *9-aoc-g198* and *9-aoc-g274* mutants display different amino acid changes in the CRISPR/Cas9 targeted 9-AOC. Local tissues included 2 cm of stem immediately surrounding the infection site. Distal stem tissues were 10 cm away and displayed no visual disease symptoms. Different letters (a–c) represent significant differences. Statistical analysis was performed using one-way ANOVA ( $P < 0.05$ ; Tukey tests were used to correct for multiple comparisons;  $P < 0.05$ ).

## Discussion

All plants are protected from biotic stress by complex and often species specific specialized metabolites that originate from the duplication and divergence conserved core biosynthetic pathways required for primary metabolism, hormone biosynthesis and growth (Moghe and Last, 2015). Similar in appearance to jasmonate hormones, maize produces a series of 9-LOX derived cyclopente(a)none death acids after pathogen attack that serve as broad cytotoxins. Established 13-AOCs in plants underlying JA biosynthesis are ineffective at cyclizing 9-LOX derived fatty acid hydroperoxide precursors, yet maize has been demonstrated to enzymatically produce 10-OPEA based on the observation of precise product stereochemistry (Christensen et al., 2015; Ogorodnikova et al., 2015). An objective of this research was to conclusively demonstrate gene(s) and enzymes responsible for the synthesis of maize death acids (10-OPEA and 10-OPDA) and ultimately gain insights into endogenous biological roles as antipathogen defenses. Maize hosts a large number of pathogenic fungal and bacterial species which cause disease and ultimately affect the yield and quality (Munkvold and White, 2016). A mechanistic understanding crop innate immunity and potential optimization of specialized metabolites that that mitigate pathogen spread will be essential to reduce yield losses from persistent biotic pressures. Related to the effort to uncover the maize 9-AOC mediated DA pathway in maize, I worked to broaden the scope of detectable GC/MS analytes. This was achieved by avoiding plastic-related chemical contamination at every step enabling a two-fold increase in the number of detectable analytes.

To connect phenotypic variation in metabolite levels to genotypic variation, fungal-elicited 10-OPEA levels were examined in genetically diverse maize stems.

Specifically the Goodman diversity panel (Flint-Garcia et al., 2005) was employed for metabolite-GWAS following Ding *et al.* (2019). In parallel the Nested Association Mapping (NAM) B73 x CML247 recombinant inbred line (RIL) subpopulation (McMullen et al., 2009) was similarly used to map loci associated with fungal-elicited 10-OPEA production. With efforts lead by Dr. Ding, the metabolite-based GWAS supported the same statistically significant region on the end of chromosome 6 near position 161,200,000 (B73 RefGen\_V3) (Fig. 1) in a region spanning approximately 70 genes. Linkage Analysis with the B73 x CML247 RILs further revealed a significant QTL in the same region. As a filter for the consideration of candidate genes in the mapping interval we examined RNA-seq based gene expression in maize leaves following challenge with SLB (Ding et al., 2019). The rationale used was that 10-OPEA and 10-OPDA are nearly undetectable in healthy tissues and are unique present in foliar tissues following fungal challenge. Using this approach, a single transcript in the mapping interval displayed a markedly increased pathogen-induced fold change (>5000) following challenge (Table 1). The B73\_refGen3 candidate gene was *GRMZM2G090245*, annotated as a germin-like protein (GLP) / Cupin domain containing protein. While cupin domain containing proteins have not been previously associated with oxylipin biosynthesis, a single protein from *Streptomyces resistomycificus* has been demonstrated to function as a cyclase in the resistomycin polyketide biosynthetic pathway (Silvennoinen et al., 2009). With the prediction that GRMZM2G090245 encoded a 9-AOC we then proceeded to create a phylogenetic tree of the B73 GPL family to consider the potential existence of related functional 9-AOC family members. RNA-seq based gene expression was further used to consider GLP family members with significant

transcript abundance following SLB challenge. Following SLB elicitation, *GRMZM2G090245* is the most highly expressed *GLP* family member in maize, displaying approximately 10-fold greater transcript levels than the next highest *GLP* (Fig. 2). From the mapping results, gene family and transcriptome analyses, we hypothesized that out of all the encoded maize GLPs, *GRMZM2G090245* might be the predominant expressed 9-AOC upon pathogen attack.

While I contributed to sample preparation for GC/MS analyses, a significant amount of the metabolite-based mapping was performed Dr. Yezhang Ding and lead to the identification 9-AOC candidate gene. Maize oxylipin biosynthetic genes and *GRMZM2G090245* were then cloned by Dr. Yezhang Ding and Mengxi Wu, for heterologous enzyme expression in tobacco using the *Agrobacterium* vector. The DA pathway conceptually parallels the JA pathway, thus any LOX enzyme capable of 9/13 dual regio-specificity with 1:1 product ratios could provide substrates to either the JA or DA pathway by producing both 9-hydroperoxides and 13-hydroperoxides. Maize LOX8 is both a 9/13 dual specific LOX and also the key maize LOX required for JA production and developmental control of pistal primordia cell death in developing tassels to yield exclusively male tissues (Acosta et al. 2009). We used maize LOX8 and the predicted allene oxide synthase AOS3 (*GRMZM2G376661*) (Borrego and Kolomiets 2016). To our knowledge, *GRMZM2G376661* / AOS3 has not been previously characterized but is a predicted functional 13-AOS. We used maize gene *GRMZM2G077316* (*AOC1*) as a 13-AOC and positive control for 12-OPDA biosynthesis in the JA pathway.

Paralleling the JA biosynthetic pathway, DA biosynthesis predictably requires 9-LOX activity on linoleic acid (18:2) or linolenic acid (18:3), the production of 9-

hydroperoxides to unstable epoxides via 9/13-AOS activity and cyclization by a 9-AOC to form cyclopentenones (Christensen et al., 2015). Maize has 13 different *LOX* genes and 5 *AOS* genes each with different product specificities and differing regiospecificity (Borrego and Kolomiets 2016). In Arabidopsis, all 4 known 13-LOX enzymes contribute to wound-induced JA biosynthesis (Chauvin et al., 2013). Given the large number of combinatorial maize LOX-AOS pairs possible and potential for additive endogenous contributions we focused on a select subset of LOX and AOS to understand 13- and 9-AOC activity. Tobacco leaf co-expression of maize LOX8, AOS3 and GRMZM2G090245 followed by 18:2 substrate feeding supported discovery of the novel 9-AOC (Fig 3a). Similarly, co-expression of maize LOX8, AOS3, and 9-AOC followed by 18:3 substrate yielded 10-OPDA. No significant 12-OPDA was formed in the presence of the maize 9-AOC consistent with a high degree of enzyme product specificity. As a positive control for 12-OPDA production, the expression of LOX8, AOS3 and AOC1 and 18:3 as a substrate resulted in significant 12-OPDA production yet no 10-OPDA (Fig. 3d and 3e). In all samples using 18:2 as substrate, low levels of 15,16-dihydro-12-oxo-phytodienoic acid were uniformly detected consistent with non-specific and non-enzymatic production in our assays (Blechert et al., 1995). By using both LOX8 as a dual regiospecific 9/13-LOX and AOS3 as a representative for 9/13-AOS, we conclude that AOC1 (13-AOC) and the novel 9-AOC represent branch points in the biosynthesis of jasmonate precursors and DAs.

In a collaboration with Dr. Bing Yang (Danforth Plant Science Center), targeted CRISPR/Cas9 mutants were created in GRMZM2G090245 to generate an endogenous 9-*aoc* mutant in the B73 inbred line (Char and Yang, 2020). Dr. Yezhang Ding and Mengxi

Wu conducted genotyping for the different types of *9-aoc* mutants resulting the absence of CRISPR/Cas9 transgenes and ultimately propagated the homozygous mutant lines. Two different *9-aoc* mutants were recovered. One *9-aoc* mutant line (g-198) represents a 4 nucleotide (NT) deletion and a 1 NT insertion that causes a single amino acid (AA) deletion followed by 10 non-synonymous AA changes amino acids near the N-terminal which finally revert back to the native sequence to produce an otherwise normal protein sequence. Early efforts to understand the 9-AOC enzyme demonstrated that small deletions near the N-terminal resulted in inactive enzymes. A second *9-aoc* mutant line (g274) resulted in non-synonymous AA changes at the same N-terminal position that continue for the entire length of the protein spanning the C-terminal.

To understand if *9-aoc* mutant(s) lead to an endogenous loss in DA production, I conducted a time course experiment in maize scutella tissues post germination where DA are known to accumulate over time and parallel increases in tissue ion leakage as a marker for cell death (Christensen et al., 2016). Scutella were analyzed from the B73 (WT) and the 11AA *9-aoc* mutation (g198) throughout a 25 day time course post germination. Maize seeds were planted 4 days apart and all plants harvested on the 25<sup>th</sup> day representing the following time points of 9, 13, 17, 21 and 25 days. Zealexins (ZX), kauralexins (KX) and dolabrallexins (DX) were additional pathway metabolites used as marker lipids for defenses from separate isoprenoid pathways (Mafu et al., 2018; Ding et al. 2019; Ding et al. 2020). For maize isoprenoid based defenses, at the final time point, there was no evidence for the biosynthetic impairment of isoprenoid defenses in the *9-aoc* mutant (Fig. 4). Predictably, we noticed significant increases in both 10-OPDA and 10-OPEA in WT B73 scutella over time (Fig. 5) consistent with previous reports

(Christensen et al., 2016). Importantly, the comparatively modest sequence mutation in the *9-aoc* g198 mutant resulted in the complete absence of 10-OPEA and 10-OPDA in endogenous scutella tissues over this same time (Fig. 5). This result supported 2 key findings. Firstly, maize appears to only have a single 9-AOC that significantly contributes to endogenous DA production. Secondly, while the non-enzymatic production of 10-OPEA from unstable allene oxides has been reported, we find no evidence that non-enzymatic production is a significant source of DA metabolites in maize tissues (Hamberg, 2000; Ogorodnikova et al., 2015).

I then focused on pathogen infection studies with the stalk rotting fungus *F. graminearum*, to examine endogenous defense responses in WT B73 plants and two different *9-aoc* mutants. SLB was further included as a pathogen and known strong elicitor of the maize DA pathway (Christensen et al., 2015). Unlike fungi such as *Fusarium verticillioides*, SLB is not significantly inhibited by high levels of 10-OPEA during *in vitro* bioassays (Christensen et al., 2015). In order to examine local DA accumulation, both fungal-infected tissues (local) and adjacent non-infected tissues (distal) were analyzed in the B73 WT and *9-aoc* mutants. As predicted, B73 WT plants accumulated significantly higher levels of both 10-OPEA (Fig 6a) and 10-OPDA (Fig 6b) in the locally infected tissues compared to non-infected distal tissues. In contrast both *9-aoc* mutants (g198 and g274) displayed significantly lower levels of 10-OPEA and 10-OPDA production (Fig. 6a and 6b). Both CRISPR/Cas9 derived *9-aoc* mutants resulted in deficient endogenous DA production in maize.

To consider if the *9-aoc* mutations resulted in the specific loss of DA and not other lipid defenses, we further analyzed zealexin levels in these same tissues. Zealexins

were first characterized in maize following the elicitation by *F. graminearum* and exist as a well characterized model for maize specific small molecule antibiotics produced as a general response to fungal attack (Huffaker et al., 2011; Ding et al., 2020). In both the *F. graminearum* and SLB infected stem tissues, total zealexin levels (sum of ZA1, ZA2, ZA6, ZB1, ZC1, ZD1) were significantly higher in g274 *9-aoc* mutant than corresponding B73 WT plants (Fig. 7). This demonstrated that the isoprenoid defensive pathways were not impaired. The higher zealexins in fungal elicited g274 *9-aoc* mutants is consistent with the presence of a greater level of pathogen infected tissues. This is a distinct prediction for *9-aoc* mutants as a direct defense, whereby loss of highly localized defense results in greater susceptibility to pathogens, more necrotic tissue and ultimately higher zealexins levels.

Based on the contributions of Dr. Yezhang Ding, Mengxi Wu and my own efforts in this project, we used genetic mapping to identify a maize gene encoding a novel 9-AOC enzyme responsible for the cyclization of fatty acid 9-allene oxides. A jasmonate pathway-like pathway in maize exists (Christensen et al., 2015; Ogorodnikova et al. 2015); however, despite 20 years of effort since the discovery of 10-OPEA and 10-OPDA in plants, no 9-AOC enzymes have been described in any biological systems (Hamberg, 2000). To date, only maize has been predicted produce 10-OPEA and 10-OPDA enzymatically and the current study supports the existence of a single enzyme. Remaining questions abound. Do other plants have the ability to use GLP enzymes to make DAs or any other oxylipins predicted to require an AOC activity (Grechkin et al., 2018)? GLP are a medium sized gene family in all grasses and have diverse dynamic rolls in both biotic and abiotic stress protection (Barman and Banerjee, 2015; Das et al.,

2019). Could GLP be the source of yet undescribed plant signals? To what extent do the maize JA and DA biosynthetic pathways interact during pathogen-induced signaling processes? Does the maize 9-AOC simply serve as a source of direct defense metabolites during pathogen-induced JA biosynthesis by LOX enzymes such as LOX8? Might 9-AOC derived DA metabolites in maize interact with the expanded maize family 4 COI receptors some of which do not appear to interact with JA (An et al., 2019)? Ultimately, the *9-aoc* mutants appear to have increased susceptibility to an evolved maize pathogen; *F. graminearum*. My Masters thesis work helped demonstrate that maize DAs such as 10-OPEA and 10-OPDA are fully enzymatic products of novel 9-AOC that makes jasmonate like cyclopentenone oxylipins as cytotoxic defenses.

## References

1. Acosta IF, Laparra H, Romero SP, Schmelz E, Hamberg M, Mottinger JP, Moreno MA, Dellaporta SL. *tasselseed1* is a lipoxygenase affecting jasmonic acid signaling in sex determination of maize. *Science*. 2009 Jan 9;323(5911):262-5. doi: 10.1126/science.1164645. PMID: 19131630.
2. An L, Ahmad RM, Ren H, Qin J, Yan Y: Jasmonate Signal Receptor Gene Family ZmCOIs Restore Male Fertility and Defense Response of Arabidopsis mutant *coil-1*. *Journal of Plant Growth Regulation* 2019, 38:479-493.
3. Alisa Huffaker, Fatma Kaplan, Martha M. Vaughan, Nicole J. Dafoe, Xinzhi Ni, James R. Rocca, Hans T. Alborn, Peter E.A. Teal, Eric A. Schmelz. *Plant Physiology* Aug 2011, 156 (4) 2082-2097; DOI: 10.1104/pp.111.179457
4. Barman AR, Banerjee J: Versatility of germin-like proteins in their sequences, expressions, and functions. *Funct Integr Genomics* 2015, 15:533-548.
5. Bleichert S, Brodschelm W, Hölder S, Kammerer L, Kutchan TM, Mueller MJ, Xia ZQ, Zenk MH: The octadecanoic pathway: signal molecules for the regulation of secondary pathways. *Proc Natl Acad Sci U S A* 1995, 92:4099-4105.
6. Block AK, Vaughan MM, Schmelz EA, Christensen SA. Biosynthesis and function of terpenoid defense compounds in maize (*Zea mays*). *Planta*. 2019 Jan;249(1):21-30. doi: 10.1007/s00425-018-2999-2. Epub 2018 Sep 6. PMID: 30187155.
7. Borrego, E. J., & Kolomiets, M. V. (2016). Synthesis and Functions of Jasmonates in Maize. *Plants (Basel, Switzerland)*, 5(4), 41. <https://doi.org/10.3390/plants5040041>
8. Char SN, Yang B: Genome editing in grass plants. *aBIOTECH* 2020, 1:41-57.
9. Chauvin A, Caldelari D, Wolfender JL, Farmer EE: Four 13-lipoxygenases contribute to rapid jasmonate synthesis in wounded *Arabidopsis thaliana* leaves: a role for

lipoxygenase 6 in responses to long-distance wound signals. *New Phytol* 2013, 197:566-575.

10. Christensen SA, Huffaker A, Hunter CT, Alborn HT, Schmelz EA: A maize death acid, 10-oxo-11-phytoenoic acid, is the predominant cyclopentenone signal present during multiple stress and developmental conditions. *Plant Signaling & Behavior* 2016, 11:5.

11. Christensen SA, Huffaker A, Kaplan F, Sims J, Ziemann S, Doehlemann G, Ji L, Schmitz RJ, Kolomiets MV, Alborn HT, Mori N, Jander G, Ni X, Sartor RC, Byers S, Abdo Z, Schmelz EA. Maize death acids, 9-lipoxygenase-derived cyclopente(a)nonenes, display activity as cytotoxic phytoalexins and transcriptional mediators. *Proc Natl Acad Sci U S A*. 2015 Sep 8;112(36):11407-12. doi: 10.1073/pnas.1511131112. Epub 2015 Aug 24. PMID: 26305953; PMCID: PMC4568653.

12. Christensen SA, Sims J, Vaughan MM, Hunter C, Block A, Willett D, Alborn HT, Huffaker A, Schmelz EA. Commercial hybrids and mutant genotypes reveal complex protective roles for inducible terpenoid defenses in maize. *J Exp Bot*. 2018 Mar 24;69(7):1693-1705. doi: 10.1093/jxb/erx495. PMID: 29361044.

13. Das A, Pramanik K, Sharma R, Gantait S, Banerjee J: In-silico study of biotic and abiotic stress-related transcription factor binding sites in the promoter regions of rice germin-like protein genes. *PLoS One* 2019, 14:e0211887.

14. de Wit PJ. How plants recognize pathogens and defend themselves. *Cell Mol Life Sci*. 2007 Nov;64(21):2726-32. doi: 10.1007/s00018-007-7284-7. PMID: 17876517.

15. Dixon RA. Natural products and plant disease resistance. *Nature*. 2001 Jun 14;411(6839):843-7. doi: 10.1038/35081178. PMID: 11459067.

16. Ding, Y., Murphy, K.M., Poretsky, E., Mafu, S., Yang, B., Char, S.N., Christensen, S., Saldivar, E., Wu, M., Wang, Q., Ji, L., Schmitz, R., Kremling, K.A., Buckler, E., Shen, Z., Briggs, S., Bohlmann, J., Sher, A.W., Castro-Falcón, G., Hughes, C., Huffaker, A., Zerbe, P., & Schmelz, E. (2019). Multiple genes recruited from hormone pathways partition maize diterpenoid defences. *Nature Plants*, 1-14.

17. Ding Y, Weckwerth PR, Poretsky E, Murphy KM, Sims J, Saldivar E, Christensen SA, Char SN, Yang B, Tong AD, Shen Z, Kremling KA, Buckler ES, Kono T, Nelson DR, Bohlmann J, Bakker MG, Vaughan MM, Khalil AS, Betsiashvili M, Dressano K, Köllner TG, Briggs SP, Zerbe P, Schmelz EA, Huffaker A. Genetic elucidation of interconnected antibiotic pathways mediating maize innate immunity. *Nat Plants*. 2020 Nov;6(11):1375-1388. doi: 10.1038/s41477-020-00787-9. Epub 2020 Oct 26. PMID: 33106639.

18. Eric A. Schmelz, Fatma Kaplan, Alisa Huffaker, Nicole J. Dafoe, Martha M. Vaughan, Xinzhi Ni, James R. Rocca, Hans T. Alborn, Peter E. Teal. *Proceedings of the National Academy of Sciences* Mar 2011, 108 (13) 5455-5460; DOI: 10.1073/pnas.1014714108

19. Flint-Garcia, S.A., Thuillet, A.-C., Yu, J., Pressoir, G., Romero, S.M., Mitchell, S.E., Doebley, J., Kresovich, S., Goodman, M.M. and Buckler, E.S. (2005), Maize association population: a high-resolution platform for quantitative trait locus dissection. *The Plant Journal*, 44: 1054-1064. <https://doi.org/10.1111/j.1365-313X.2005.02591.x>

20. Grechkin AN, Ogorodnikova AV, Egorova AM, Mukhitova FK, Ilyina TM, Khairutdinov BI: Allene Oxide Synthase Pathway in Cereal Roots: Detection of Novel Oxylipin Graminoxins. *ChemistryOpen* 2018, 7:336-343.

21. Hamberg M: New cyclopentenone fatty acids formed from linoleic and linolenic acids in potato. *Lipids* 2000, 35:353-363.

22. Huang AC, Osbourn A. Plant terpenes that mediate below-ground interactions: prospects for bioengineering terpenoids for plant protection. *Pest Manag Sci*. 2019 Sep;75(9):2368-2377. doi: 10.1002/ps.5410. Epub 2019 Apr 8. PMID: 30884099; PMCID: PMC6690754.

23. Huffaker A, Kaplan F, Vaughan MM, Dafoe NJ, Ni X, Rocca JR, Alborn HT, Teal PE, Schmelz EA. Novel acidic sesquiterpenoids constitute a dominant class of pathogen-induced phytoalexins in maize. *Plant Physiol*. 2011 Aug;156(4):2082-97. doi: 10.1104/pp.111.179457. Epub 2011 Jun 20. PMID: 21690302; PMCID: PMC3149930.

24. Kelman, Arthur , Pelczar, Michael J. , Pelczar, Rita M. and Shurtleff, Malcolm C.. "Plant disease". *Encyclopedia Britannica*, 1 Apr. 2020, <https://www.britannica.com/science/plant-disease>. Accessed 18 May 2021.

25. McMullen MD, Kresovich S, Villeda HS, Bradbury P, Li H, Sun Q, Flint-Garcia S, Thornsberry J, Acharya C, Bottoms C, Brown P, Browne C, Eller M, Guill K, Harjes C, Kroon D, Lepak N, Mitchell SE, Peterson B, Pressoir G, Romero S, Oropeza Rosas M, Salvo S, Yates H, Hanson M, Jones E, Smith S, Glaubitz JC, Goodman M, Ware D, Holland JB, Buckler ES. Genetic properties of the maize nested association mapping population. *Science*. 2009 Aug 7;325(5941):737-40. doi: 10.1126/science.1174320. PMID: 19661427.
26. Moghe GD, Last RL: Something Old, Something New: Conserved Enzymes and the Evolution of Novelty in Plant Specialized Metabolism. *Plant Physiology* 2015, 169:1512-1523
27. Munkvold GP, White DG: Compendium of corn diseases, vol 165: Am Phytopath Society; 2016.
28. Ogorodnikova AV, Gorina SS, Mukhtarova LS, Mukhitova FK, Toporkova YY, Hamberg M, Grechkin AN. Stereospecific biosynthesis of (9S,13S)-10-oxo-phytoenoic acid in young maize roots. *Biochim Biophys Acta*. 2015 Sep;1851(9):1262-70. doi: 10.1016/j.bbaliip.2015.05.004. Epub 2015 May 22. PMID: 26008579.
29. Pelczar, Rita M. , Shurtleff, Malcolm C. , Kelman, Arthur and Pelczar, Michael J.. "Plant disease". *Encyclopedia Britannica*, 1 Apr. 2020, <https://www.britannica.com/science/plant-disease>. Accessed 18 May 2021.
30. Schmelz, E.A., Engelberth, J., Tumlinson, J.H., Block, A. and Alborn, H.T. (2004), The use of vapor phase extraction in metabolic profiling of phytohormones and other metabolites. *The Plant Journal*, 39: 790-808. <https://doi.org/10.1111/j.1365-313X.2004.02168.x>
31. Schmelz EA, Huffaker A, Sims JW, Christensen SA, Lu X, Okada K, Peters RJ. Biosynthesis, elicitation and roles of monocot terpenoid phytoalexins. *Plant J*. 2014 Aug;79(4):659-78. doi: 10.1111/tpj.12436. Epub 2014 Mar 26. PMID: 24450747.
32. Sibongile Mafu, Yezhang Ding, Katherine M. Murphy, Omar Yaacoobi, J. Bennett Addison, Qiang Wang, Zhouxin Shen, Steven P. Briggs, Jörg Bohlmann, Gabriel Castro-

Falcon, Chambers C. Hughes, Mariam Betsiashvili, Alisa Huffaker, Eric A. Schmelz, Philipp Zerbe, Discovery, Biosynthesis and Stress-Related Accumulation of Dolabradiene-Derived Defenses in Maize , *Plant Physiology*, Volume 176, Issue 4, April 2018, Pages 2677–2690, <https://doi.org/10.1104/pp.17.01351>

33. Silvennoinen L, Sandalova T, Schneider G: The polyketide cyclase RemF from *Streptomyces resistomycificus* contains an unusual octahedral zinc binding site. *FEBS Lett* 2009, 583:2917-2921.

34. War, A. R., Paulraj, M. G., Ahmad, T., Buhroo, A. A., Hussain, B., Ignacimuthu, S., & Sharma, H. C. (2012). Mechanisms of plant defense against insect herbivores. *Plant signaling & behavior*, 7(10), 1306–1320. <https://doi.org/10.4161/psb.21663>

35. Yan Y, Christensen S, Isakeit T, Engelberth J, Meeley R, Hayward A, Emery RJ, Kolomiets MV. Disruption of OPR7 and OPR8 reveals the versatile functions of jasmonic acid in maize development and defense. *Plant Cell*. 2012 Apr;24(4):1420-36. doi: 10.1105/tpc.111.094151. Epub 2012 Apr 20. PMID: 22523204; PMCID: PMC3398555.